Lab on a Chip

Cite this: *Lab Chip*, 2012, **12**, 503

www.rsc.org/loc

HIGHLIGHT

Research highlights

Šeila Selimović[ab] and Ali Khademhosseini*[abcd]

DOI: 10.1039/c1lc90140k

Hybridoma: on-chip cell fusion

Antibodies have been used for many different applications ranging from basic biological studies to therapeutics. For example, antibodies are used in treatments as wide ranging as cancer care, autoimmune disease therapy, and to prevent rejection of transplanted organs.[1] This requires large quantities of antibodies, which can be supplied *via* hybridoma generation. Hybridomas are hybrid cell lines formed *via* electrofusion from B-cells that produce a specific antibody, and immortalized B-cell cancer cells (myelomas).[2] The fused cells can then be triggered to express large quantities of the required antibodies.

The yield of fused cells as well as the yield of functional hybridomas is very low in standard bench-scale techniques. To address this challenge van den Berg and colleagues developed a microscale device that helped them significantly increase the number of active hybridomas. The poly(dimethylsiloxane) (PDMS) device engineered by Kemna *et al.*[3] incorporated an array of ~800 cell traps, placed between two Pt electrodes (Fig. 1). The traps were designed to hold a 7.5 μm large human B-cell and a 15 μm large mouse myeloma cell each. The largest fraction of pairing between these two cell types was ~33% and was found to depend on the spacing between adjacent traps.

To fuse the cell pairs, a series of six 100 μs DC pulses at 2.5 kV cm^{-1} was applied. To maintain high cell viability in such strong electric fields, pronase was added to the cells to strengthen the cell membranes. Interestingly, when shorter pulses (50 μs) were used, the membrane stabilizing effect of pronase was too strong to allow for fusion. In some cases, an AC field was applied for 30 s at 2 MHz, prior to and after the DC pulses. The efficiency of initial fusion (dye transfer) in those experiments reached 40%, when 6 long instead of 3 short DC pulses were used. Similarly, advanced fusion, which refers to the membrane reorganization, also had higher success rates, roughly 10% compared to ~1%.

The final step in the cell fusion process is nuclear fusion, which takes place up to 3 weeks later. At this point roughly 1.2% of the loaded cell pairs formed viable hybridomas. While this fraction seems low, it constitutes a significant improvement to bulk electrofusion, which usually yields only 0.001% active hybridomas. Thus, the application of microfluidics to pair and fuse individual cells of different types could potentially greatly benefit hybridoma and ultimately antibody generation. To improve the usefulness of the device, the authors could in the future consider a modified trap array, designed to hold tens of thousands of cell pairs. Furthermore, the ultimate test of this technique, namely the analysis of the produced antibody, is yet to be completed. However, there is no indication that the microfluidic environment should affect this facet of the hybridoma activity.

Lab in a tube

Many biological analysis techniques rely on invasive actions, such as transfection of cells to stimulate expression of fluorescent proteins, direct labeling of cells, bacteria and viruses with fluorescent markers, or cell lysis to collect and study the cell contents. By subjecting their samples to these analysis methods researchers potentially alter the sample and the test products. Thus, there has been interest in developing non-invasive and label-free, yet fast and affordable, high throughput approaches to investigate biological samples.

Optical microcavity resonators (OCRs) offer such opportunities, especially since they are compatible with microscale fabrication technologies and fluidic and capillary systems. OCRs are microscale structures that facilitate almost total internal reflection of light at resonant frequencies.[5,6] Recently, Schmidt and coworkers have shown that such microresonators could be used to efficiently trap and sense individual cells in an optofluidic setup.

Smith *et al.*[4] developed an array of microcavities on a quartz surface, fabricated from 42 nm thick SiO/SiO_2 nanomembranes that rolled into cylinders. Each cylinder had ~1.5 windings and a nanosized gap between them. When the array was embedded into a medium-containing petri dish, a microcapillary was used to stick individual NIH 3T3 fibroblasts into each microcavity from the medium (Fig. 2). Since these cells are soft, it was possible to capture cells whose diameter was up to 2.3 times larger than that of the cavity (6–10 μm). In most cases the cells only filled one half of the cavity and protruded into the medium.

[a]*Center for Biomedical Engineering, Department of Medicine, Brigham and Women's Hospital, Harvard Medical School, Cambridge, Massachusetts 02139, U. S. A. E-mail: alik@rics.bwh.harvard.edu*
[b]*Harvard-MIT Division of Health Sciences and Technology, Massachusetts Institute of Technology, Cambridge, Massachusetts 02139, U. S. A.*
[c]*Wyss Institute for Biologically Inspired Engineering, Harvard University, Boston, Massachusetts 02115, U. S. A.*
[d]*World Premier International–Advanced Institute for Materials Research (WPI-AIMR), Tohoku University, Sendai 980-8577, Japan*

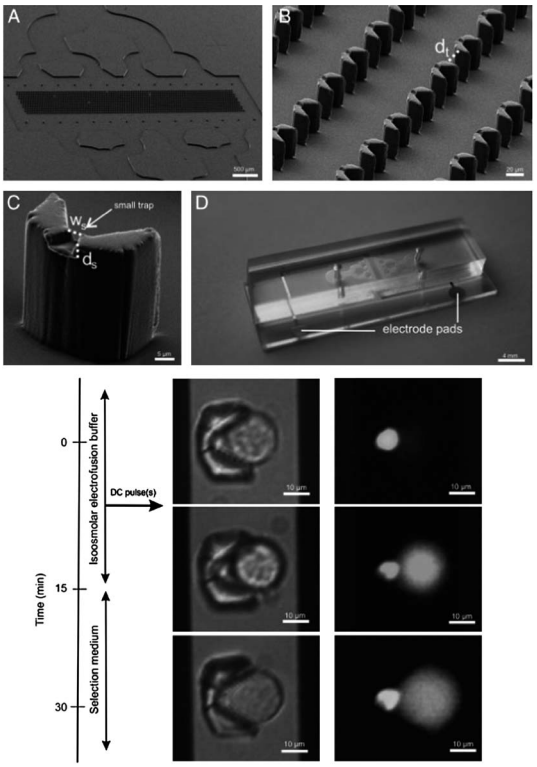

Fig. 1 Top: SEM images of the cell electrofusion chip: (a) PDMS device, (b) part of the trap array, (c) single trap, and (d) full device including the electrodes. Bottom: Phase contrast and fluorescence photographs indicating different stages of cell fusion and reorganization after exposure to an electric field. The fluorescent dye contained in the smaller B-cell is distributed throughout both cells after electrofusion. Figure adapted and reprinted with permission from Kemna *et al.*[3]

Micro-photoluminescence analysis of the cavities at 442 nm (HeCd laser) indicated that the chief whispering gallery modes (WGM) were transverse-magnetic, while transverse-electric modes were attenuated. In addition, the empty cavity ends had blue-shifted WGM spectra compared to cavities filled with a cell. However, the cavity ends in which cells were captured generated spectra with peaks at the same wavelengths, regardless of the presence of a cell. This sensing response was effected by the physical changes in the microresonator upon the introduction of a cell. Namely, the cavity end which housed the cell became distended and the nanogap between the cylinder windings decreased. The same nanogap reduction was observed at the empty end. In both cases, the smaller nanogap led to better reflection of light and thus a smaller energy loss and a higher quality factor. Further, the empty end became more compact as the cylinder tightened. This reduction in cavity diameter led to a blue shift in the WGMs.

The sensing capability of the microcavities, expressed in terms of the quality factor, was shown to diminish after the capture and removal of the first cell. This was due to a hysteresis effect in the cavity, where the nanogap did not fully widen to its original shape. However, after the trapping and ejection of a second cell the quality factor had roughly constant values in empty and filled cavities.

These observations indicate that the WGMs and the quality factor depend on the nanogap size and therefore on the size and stiffness of the captured cells. Thus, it would be helpful to utilize the nanogap microcavity resonator array to measure stiffness changes in cells exposed to various growth factors and toxins. This would be facilitated by surface modifying the microcavity, a process already successfully conducted by the same authors, and keeping cells captured for an extended amount of time. It remains unclear how the presented sensing technique could be joined with 3D tissue culture, yet such an application would make the microcavity resistor appealing to a wider variety of fields.

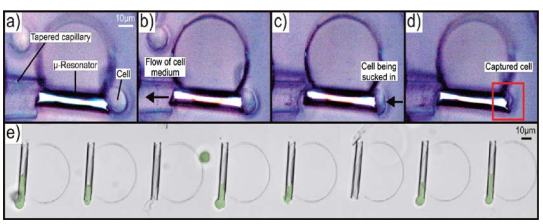

Fig. 2 Time-sequence images of a mouse fibroblast being captured inside a microresonator by a capillary (a–d); a series of cell-laden resonators (e). Figure reprinted with permission from Smith *et al.*[4]

Soft grayscale lithography for chemical gradients

Self-assembled monolayers (SAMs) are used in engineering applications (controlled surface patterning), chemistry (chemical sensing) and biological studies (cell behavior on different substrates). These applications require different chemical and physical properties of the SAM such as spatial organization of the resulting monolayer. Methods that allow for the formation of SAMs with varying spatial properties, or SAM gradients, include solution and vapor diffusion, selective material ablation and local molecule desorption *via* laser on one hand and high-precision grayscale lithography (GL) on the other hand.[7] GL utilizes sub-resolution mask patterns to modify the intensity of UV light incident on photosensitive molecules, which provides patterns of different functional groups.

Nuzzo and colleagues have recently introduced a grayscale patterning method for chemical gradients based on a PDMS mask. Instead of using a transparency mask, Bowen *et al.*[8] created a series of masking channels in a PDMS device on a Kapton substrate and filled them with different mixtures of clear and carbon-black filled PDMS (bPDMS). The higher the proportion of bPDMS, the more

opaque the channel filling. To create a positive grayscale mask, the cured PDMS device was removed from the substrate, such that it was transparent aside from the bPDMS filled channels. To create a negative grayscale mask, the device was originally bonded to a thin layer of PDMS coated with an optically dense layer of gold. Gold etch was first flushed through the channels to remove the gold underneath them, then the channels were filled with PDMS as described above. The result was an opaque device with transparent windows underneath the mask channels.

To test the quality of the device the authors created a gradient of photosensitive coumarin. A major benefit of this material was that it did not release reactive species upon UV exposure and its modification could therefore be precisely controlled. Further, photocleavage of coumarin exposed terminal sulfonic groups, which lowered the hydrophobicity of the SAM. Exposing coumarin through a high-volume fraction bPDMS mask had a similar effect as a short exposure time through a fully transparent mask. Namely, the SAM had a large contact angle. On the contrary, exposing the layer through a low-volume fraction bPDMS mask decreased the contact angle of the coumarin film, just like exposing the film for a long time to UV light. In summary, the more sulfonic acid groups were revealed, the lower the contact angle of the coumarin SAM.

In another device, the variable SAM wettability was utilized for a microfluidic study of a passive gating system. Here, a single fluidic channel was superposed on five SAM zones with different contact angles. When pressure driven flow of water was applied in the channel, the water stream only filled one channel zone at a time. In order for water to enter a zone with a higher contact angle, a higher pressure was required to drive the fluid. Thus, the different zones had different threshold pressures and could therefore be considered temporary valves or gates.

The main benefit of the present chemical gradient fabrication method is its low cost. Since the technique only relies on a PDMS mask and a UV source, no expensive equipment is necessary. Furthermore, using photocleavable SAM offers high precision in separating different regions of the treated SAM, compared to post-processing the material with laser or to diffusion-based gradient. Lastly, the resolution of grayscale lithography as presented here is compatible with microfluidic applications and the method can be used to fabricate novel microfluidic elements. In the future, devices fabricated using this technique could be useful for tissue engineering applications, especially if biocompatible materials like coumarin, which do not produce free radicals, are used. In this context it would be worthwhile to combine topographical SAM diversity with the produced chemical and physical gradients, *e.g.*, for studies of different cell microenvironments.

References

1 P. J. Carter, Potent antibody therapeutics by design, *Nat. Rev. Immunol.*, 2006, **6**(5), 343–357.
2 G. Köhler and C. Milstein, Continuous cultures of fused cells secreting antibody of predefined specificity, *Nature*, 1975, **256** (5517), 495–497.
3 E. W. M. Kemna, *et al.*, On chip electrofusion of single human B cells and mouse myeloma cells for efficient hybridoma generation, *Electrophoresis*, 2011, **32**, 3138–3146.
4 E. J. Smith, *et al.*, Lab-in-a-Tube: Detection of Individual Mouse Cells for Analysis in Flexible Split-Wall Microtube Resonator Sensors, *Nano Lett.*, 2011, **11**, 4037–4042.
5 A. M. Armani, *et al.*, Label-Free, Single-Molecule Detection with Optical Microcavities, *Science*, 2007, **317**(5839), 783–787.
6 K. J. Vahala, Optical microcavities, *Nature*, 2003, **424**(6950), 839–846.
7 J. C. Huie, Guided molecular self-assembly: a review of recent efforts, *Smart Mater. Struct.*, 2003, **12**(2), 264–271.
8 A. M. Bowen, *et al.*, Programmable Chemical Gradient Patterns by Soft Grayscale Lithography, *Small*, 2011, **7**, 3350–3362.